Griffiths phase and thermomagnetic irreversibility behavior in slightly electron-doped manganites Sm$_{1-x}$Ca$_x$MnO$_3$ ($0.80 \leq x \leq 0.92$)

P. Tong,[1,2] Bongju Kim,[1] Daeyoung Kwon,[1] T. Qian,[1] Sung-Ik Lee,[3,4] S-W. Cheong,[5] and Bog G. Kim[1]

[1]*Department of Physics and Research Center for Dielectric and Advanced Matter Physics, Pusan National University, Busan 609-735, Republic of Korea*

[2]*Key Laboratory of Materials Physics, Institute of Solid State Physics, and Hefei High Magnetic Field Laboratory, Chinese Academy of Sciences, Hefei 230031, People's Republic of China*

[3]*Department of Physics, Sogang University, Seoul 121-742, Republic of Korea*

[4]*National Creative Research Initiative Center for Superconductivity, Pohang University of Science and Technology, Pohang 790-784, Republic of Korea*

[5]*Department of Physics and Astronomy and Rutgers Center for Emergent Materials, Rutgers University, Piscataway, New Jersey 08854, USA*

We report the magnetic properties of slightly electron-doped Sm$_{1-x}$Ca$_x$MnO$_3$ ($0.80 \leq x \leq 0.92$). The Griffiths phase behavior in the inverse magnetic susceptibility was observed for $x \geq 0.85$. The thermomagnetic irreversibility found in all samples could be explained according to the influence of martensitic strain on the magnetization behavior under various cooling histories. In the modified phase diagram, the low-field thermomagnetic irreversibility line passes through the region of Griffiths phase, indicating that the Griffiths phase is correlated with the accommodation strain. Our result indicates that the strain field, in addition to quenched disorders, may be an alternative approach to understand the observed Griffiths phase. Besides, the Griffiths phase itself is suggested to be insufficient for the appearance of colossal magnetoresistance effect in the present system.

I. INTRODUCTION

Perovskite manganites have attracted considerable attention since the discovery of the colossal magnetoresistance (CMR) effect.[1] Understanding the mechanism of the CMR effect is very important both theoretically and practically.[2] Recently, the phase separation, typically involving ferromagnetic (FM) metallic and antiferromagnetic (AFM) charge and orbital ordered insulating domains, has been confirmed to be intrinsic and crucial to comprehend the CMR effect and the related properties in manganites.[3] Usually, the phase coexistence in nanometer and/or micrometer scale has been believed to originate from various reasons, such as disorder by chemical doping and the random field.[3] An alternative mechanism for the phase separation and the related issues was proposed without explicit disorder, which shows that both nanometer- and micrometer-scale multiphase coexistences are self-organized and caused by the presence of an intrinsic elastic energy landscape (strain field).[4] Accordingly, recent experiments accumulated to emphasize the important roles of the accommodation strain in determining the unique properties of manganites, such as phase separation, glassy state, metal-insulator transition, percolation behavior, magnetic field history dependent magnetization and steps in magnetization, and resistivity.[5,6]

The Griffiths phase was first proposed by Griffiths[7] to explain the effects of the quenched randomness on the magnetization of a dilute Ising ferromagnet. The Griffiths phase means the existence of short-range ordering of FM clusters in a paramagnetic (PM) matrix when $T_C \leq T \leq T_G$. Here, T_G is the characteristic temperature at which the FM clusters begin to nucleate, while T_C represents for the FM Curie temperature. The seeds for FM clusters to nucleate are usually considered to be the quenched disorders which can be enhanced by the competition between the phases.[8] The Griffiths phase behavior has been widely observed in various systems, including heavy Fermi materials,[9] spin glass systems,[10] hole-doped perovskite manganites,[11–14] and layered manganites.[15] However, the Griffiths phase behavior was rarely reported in the electron-doped manganites.[16,17] Moreover, there is a debate lunched recently on whether the Griffiths phase is always a precursor to CMR in manganites or not.[11,13,15]

Here, we report the observation of Griffiths phase via magnetization measurement in the electron-doped manganites Sm$_{1-x}$Ca$_x$MnO$_3$ with $x \geq 0.85$. The thermomagnetic irreversibility (TMI) behavior was also observed in all samples with $0.80 \leq x \leq 0.92$, which indicates the existence of accommodation strain. A modified phase diagram was established, in which the TMI line locates well in the region of Griffiths phase when $x \geq 0.85$. Our result suggests that the origin of Griffiths phase is probably associated with the accommodation strain. From this phase diagram, it is also suggested that the Griffiths phase is not always accompanied by a CMR effect in the electron-doped manganites.

II. EXPERIMENT

The polycrystalline Sm$_{1-x}$Ca$_x$MnO$_3$ ($0.80 \leq x \leq 0.92$) samples were synthesized from the stoichiometric mixture of the predried Sm$_2$O$_3$, CaCO$_3$, and MnO$_2$ powders by solid-state reaction method with the similar heat treatment as reported in Ref. 18. The x-ray powder diffraction (XRD) patterns at various temperatures were recorded by D8 Advance diffractometer with a Lynxeye detector using Cu $K\alpha$ radiation. The analysis of the crystal structure by Rietveld refinement using FULLPROF program was performed. Magnetiza-
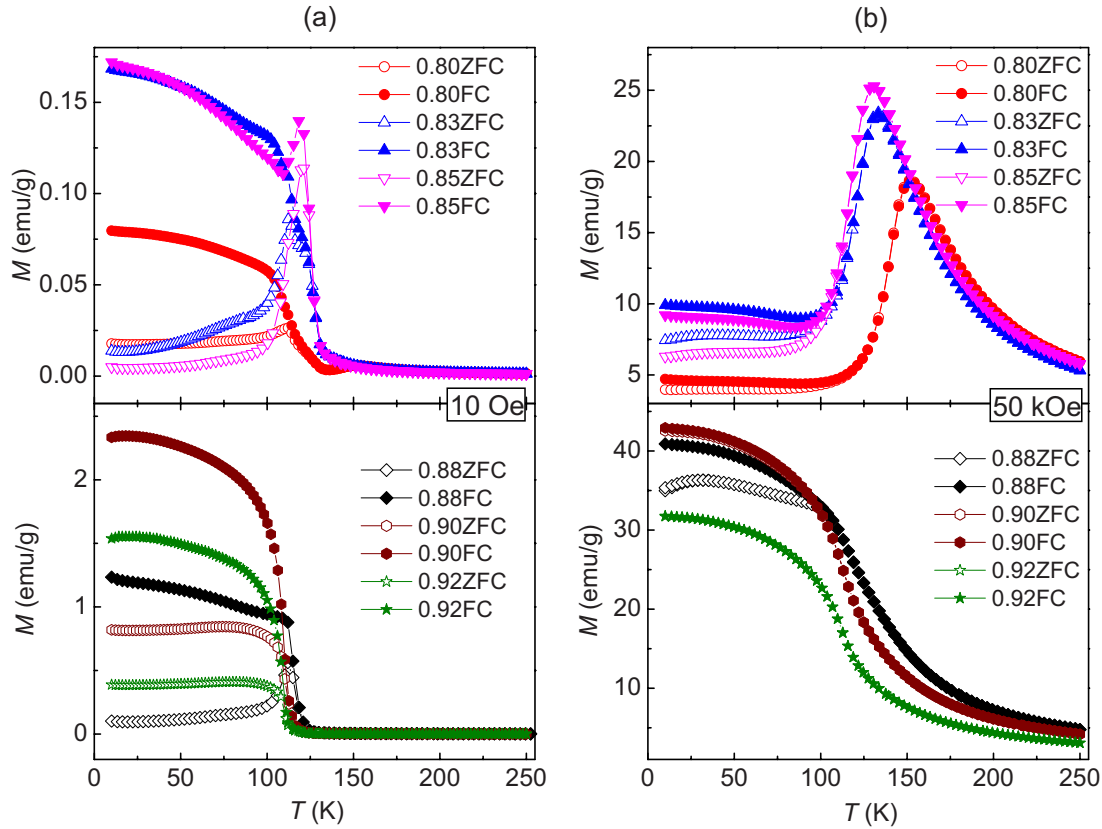
FIG. 1. (Color online) $M(T)$ curves measured at (a) $H=10$ Oe and (b) 50 kOe.

tion measurements were carried out with superconducting quantum interference device magnetometer (MPMS, Quantum Design). The temperature dependent magnetization $M(T)$ in the temperature range 10 K $\leq T \leq$ 250 K under 10 Oe and 50 kOe and field dependent magnetization $M(H)$ at 10 K up to 50 kOe were measured in the zero-field-cooled (ZFC) and field-cooled (FC) conditions. If not specially emphasized, "FC" in this article means applying a certain external field to the samples at room temperature and then cooling to the low temperatures under the same field.

III. RESULTS AND DISCUSSION

A. Griffiths phase

Figure 1 shows $M(T)$ ($10 \leq T \leq 300$ K) measured at both 10 Oe and 50 kOe for $Sm_{1-x}Ca_xMnO_3$ ($0.80 \leq x \leq 0.92$) under both ZFC and FC modes. In Fig. 1(a), the peaks in ZFC-$M(T)$ curves for $x \leq 0.85$ correspond to the C-type AFM (C-AFM) transition temperature $T_N(C)$. Above x $=0.85$, the FC-$M(T)$ curves take on a shape of FM behavior, thus, T_C can be determined as the reflection point of $dM(T)/dT$. In this composition range, the FM transition has been testified to be accompanied by a G-type AFM (G-AFM) transition, namely, $T_C \sim T_N(G)$.[19] As a result, $T_N(C)$ decreases from 152 K for $x=0.80$ to 120 K for $x=0.85$. For samples with $x \geq 0.85$, $T_C \sim T_N(G)$ equals to ~ 110 K. It should be noted that T_C (~ 115 K) obtained by $dM(T)/dT$ for $x=0.85$ means the onset of a short-range FM order, not

that of a long-range one, as will be demonstrated in the following text.

The inverse dc susceptibility $1/\chi(T)$ deduced from ZFC-$M(T)$ at 10 Oe was plotted in Figs. 2(a) and 2(b). For all samples, the high-temperature curve follows the Curie–Weiss law, i.e., $1/\chi(T)$ is linearly dependent on the temperature. The curve for sample $x=0.80$ displays a broaden peak at 130 K, which is relevant to the C-AFM correlations below $T_N(C)$. The relative peak is very weak in $x=0.83$ curve. In contrast, for $x \geq 0.85$, all $1/\chi(T)$ curves exhibit a Griffiths phaselike downturn below a certain temperature. The onset of this downturn is denoted as T_G (i.e., the temperature where $1/\chi(T)$ deviates from the Curie–Weiss behavior) below which the FM clusters emerge in the PM matrix, as is described in a Griffiths phase system.[20] The determined T_G for samples with $x \geq 0.85$ decreases slightly with an increasing x.

In order to get a further insight into this kind of abnormal behavior of inverse susceptibility for $x \geq 0.85$, the measurement of field dependent dc magnetic susceptibility $\chi(T)$ in ZFC mode was performed. As an example, Fig. 2(c) shows the result for $x=0.90$. It is apparent that increasing applied field gradually suppresses the downturn behavior in $1/\chi(T)$ curve. Eventually, as shown in the inset of Fig. 2(c), $1/\chi(T)$ measured at 50 kOe reveals a typical Curie–Weiss behavior above T_C. The $1/\chi(T)$ for $x=0.90$ at both 10 Oe and 50 kOe were redrawn in Fig. 2(d) in the *log-log* form. There exists a noticeable singularity between the Griffiths and high-temperature PM phases in 10 Oe curve. The data in the Griffiths phase was tentatively fitted using the expression χ^{-1}
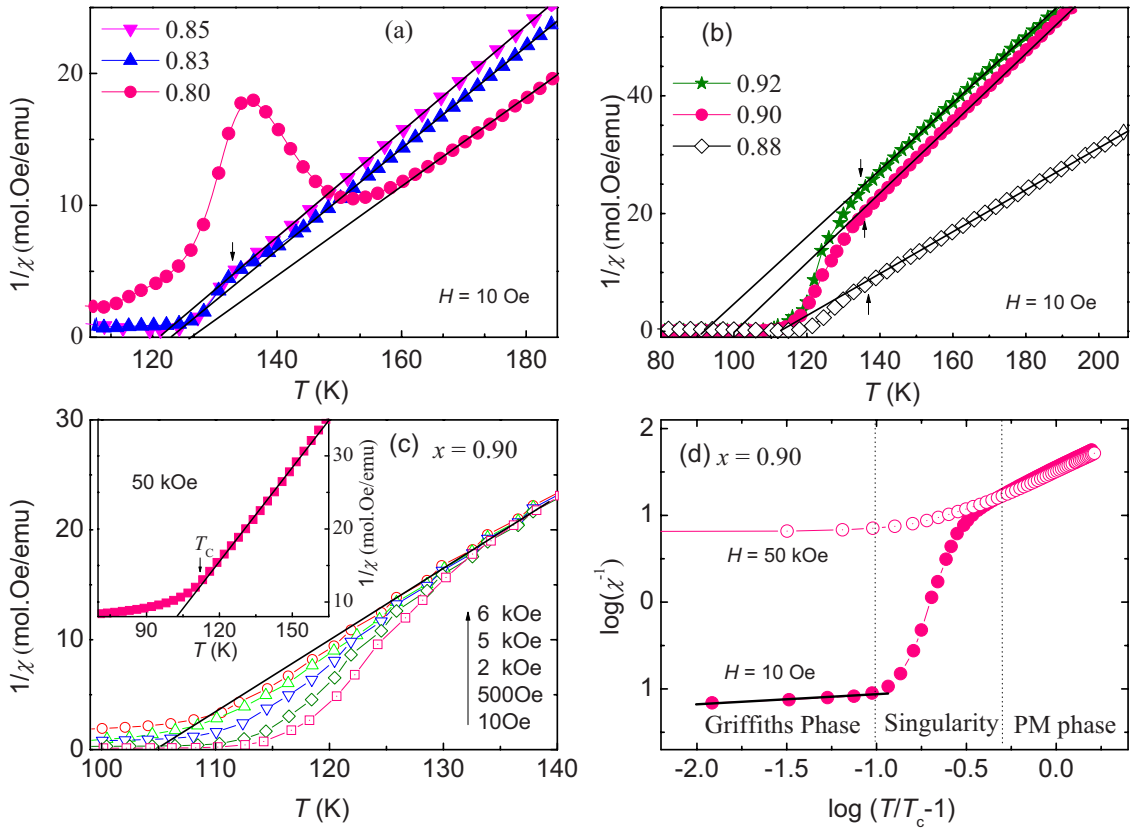
FIG. 2. (Color online) Inverse dc magnetic susceptibility $1/\chi(T)$ for (a) $x=0.80$, 0.83, 0.85 and (b) $x=0.88$, 0.90, 0.92. Solid lines indicate a Curie–Weiss behavior. Arrows indicate the Griffiths temperature T_G (see text for its detailed definition). (c) $1/\chi(T)$ under various magnetic fields for $x=0.90$. The data with $H=50$ kOe is plotted in the inset. Solid lines are the expected Curie–Weiss behavior. (d) The $\log(\chi-1)$ vs $\log(T/T_C-1)$ plots for $x=0.90$ at $H=10$ Oe and 50 kOe. Solid line indicates a linear fitting.

$\propto (T-T_C)^{1-\lambda}$, where λ is the magnetic susceptibility exponent.[9] The estimated exponent λ is about 0.85, which is in good agreement with the expected range $0 \leq \lambda \leq 1$.[9] This singularity, however, is smeared out in the 50 kOe curve. In the sense of Griffiths phase, the suppression of this kind of singularity under external field is due to the hindering of the small FM signal by increasing the background PM signal and/or the saturation of the FM component with increasing external field.[20] As a result, the abnormal downturn behavior in $1/\chi(T)$ curves for $x \geq 0.85$ could be ascribed to the existence of Griffiths phase.

B. Thermomagnetic irreversibility

A significant divergence between ZFC- and FC-$M(T)$ curves under 10 Oe at low temperatures can be found in Fig. 1(a) for all samples, indicating a TMI behavior. The temperature where ZFC- and ZFC-$M(T)$ departs from each other is defined as the irreversibility temperature T_{irr} which is nearly constant (~ 126 K) at 10 Oe for all samples. At 50 kOe, however, T_{irr} is strongly decreased and the ZFC-$M(T)$ coincides well with FC-$M(T)$ for $x \geq 0.90$.

The TMI behavior is generally related to a spin glass or a cluster glass.[21] Fundamentally, the cluster glass can be regarded as a type of spin glass.[4,22] Here, we will not distinguish one from other in details. Here, T_{irr} at 10 Oe is remark-

ably above T_C for $x \geq 0.85$. This is unlike the case of a conventional cluster glass or spin glass, in which low-field T_{irr} is well below or just below T_C.[22] The absolute and relative differences between FC-$M(10$ K) and ZFC-$M(10$ K) [i.e., $M_{FC}-M_{ZFC}$ and $(M_{FC}-M_{ZFC})/M_{ZFC}$, respectively] under both 50 kOe and 10 Oe are plotted in Fig. 3. One can see that $M_{FC}-M_{ZFC}$ for middle Ca composition is much larger at 50 kOe than at 10 Oe [Fig. 3(a)]. In contrast, as shown in Fig. 3(b), $(M_{FC}-M_{ZFC})/M_{ZFC}$ at 50 kOe is lower than that at 10 Oe in the whole composition range studied.

A significant difference between FC and ZFC modes was also found in $M(H)$ for $x=0.85$ as shown in Fig. 4(a). Similar phenomenon exists in sample with $x=0.88$ (not shown here) but disappears in other samples, e.g., $x=0.92$ as shown in Fig. 4(a) as a comparison. This result is consistent with Ref. 19. In Ref. 19, the authors attributed this behavior to an increase in FM fraction after field cooling from room temperature. Here, what we would like to emphasize is that the value of $M_{FC}-M_{ZFC}$ in $M(H)$ under 50 kOe is strongly dependent on the temperature T^*, from which the magnetic field is applied and the sample is cooled down to lower temperatures under this field. The case of $x=0.88$ is displayed in Fig. 4(b). A sudden reduction in $M_{FC}-M_{ZFC}$ is found at T^* ~ 100 K, which is close to its phase transition temperature, namely T_C [$\sim T_N(G)$]. When T^* is larger than 100 K, $M_{FC}-M_{ZFC}$ modestly increases with increasing T^*.
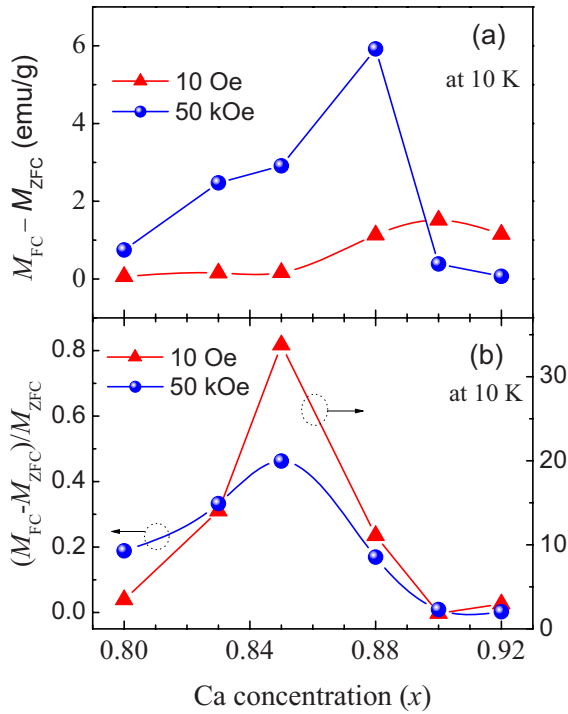
FIG. 3. (Color online) x dependent (a) $M_{FC}-M_{ZFC}$ and (b) $(M_{FC}-M_{ZFC})/M_{ZFC}$ at 10 K, deduced from $M(T)$ under $H=10$ Oe and 50 kOe.

The cooperation of structural and magnetic phase transitions would play a key role in determining the properties in present system. For the extensively studied composition $x=0.85$, it changes from an orthorhombic ($Pnma$) PM state at high temperatures to a phase separated system below T_C, i.e., orthorhombic G-AFM plus monoclinic ($P2_{1/m}$) C-AFM. Simultaneously, FM clusters are embedded in the G-AFM matrix.[18,19] In the monoclinic phase, the MnO_6 octahedra are strongly distorted, namely, elongated along the FM rows of the C-AFM structure. Since the new monoclinic phase is more distorted than its parent orthorhombic phase, the strain along the grain boundaries of remained orthorhombic phase would be accommodated below the structure transition temperature as observed in a martensitic phase transition.[23–27]

With the decreasing temperature, the accommodation strain will grow, resulting in the establishment of the thermal-elastic equilibrium between the parent phase and the martensite phase. Such a strain may lead to the energy barriers that inhibit further growth of coexisting FM or AFM component and stabilize the large-scale phase separation. In fact, a twinning microstructure, which is frequently observed after a martensitic phase transition,[28] has been detected in samples with $x=0.85$ and 0.90 at low temperatures.[29]

In terms of accommodation strain, the decrease in $M_{FC}-M_{ZFC}$ in $M(H)$ with decreasing T^* can be attributable to the increasing strength of the strain accommodation with lowering temperature, which hinders the expansion of the orthorhombic phase in low temperature, hence, the increase in the FM fraction. Thus, the lower the T^* is, the more difficult for the FM fraction to increase and to survive at low temperatures. Above the phase transition temperature, the strain even if exists should be very weak. Moreover, the FM clusters at

high temperature clusters indicated by the Griffiths phase behavior would align to the direction of the field and/or grow in size under the external field. It is beneficial to the enhancement of FM fraction and its survival at lower temperatures. So the value of $M_{FC}-M_{ZFC}$ is considerably high and nearly independent of T^* when T^* is above the phase transition temperature.

As shown in Fig. 4(c) we can see that the monoclinic phase fraction f_M obtained from the refinement of XRD data is neglectably low for $x \geq 0.90$ at 80 K, while suddenly increases to $x=0.88$ and shows a tendency to be saturated with further decreasing x. This evolution of f_M with x will be helpful to understand the composition dependent TMI behavior of $M(T)$ as summarized in Fig. 3.

Figure 4(d) displays the Arrott plots for $x=0.85$, 0.88, and 0.92. For $x=0.85$, the linear extrapolation of high-field portion of the Arrott plot to $H/M=0$ yields a negative intercept on M^2 axis, indicating the absence of spontaneous magnetization and long-range FM ordering. In contrast, for $x=0.88$ and 0.92, the Arrott plot indicates the existence of long-range FM correlation because of a positive intercept on M^2 axis. At the side of $x=0.8$, the orthorhombic phase is surrounded by the dominant C-AFM phase, so that the movement and growth of FM clusters will be strongly hindered by its surroundings via the strain accommodation. Furthermore, the Griffiths phase is weak or absent in them. All these indicate a very small FM fraction added into the sample after the process of field cooling under $H=50$ kOe. Therefore, $M_{FC}-M_{ZFC}$ is weak on $x=0.80$ side, as shown in Fig. 3(a).

On the other side, i.e., in $x=0.92$, the orthorhombic phase is dominant, in accordance with a long-range FM background. Keeping in mind that the additional orthorhombic FM fraction after FC process originates from the monoclinic phase which is nearly absent on the side of 0.92, field cooling from high temperature will produce a very small amount of FM fraction, hence, a small value of $M_{FC}-M_{ZFC}$. In samples with middle Ca content such as $x=0.85$ and 0.88, below $T_N (C)$, a subtle balance between the orthorhombic FM and monoclinic C-AFM domains comes into being with a weak energy barrier of the accommodated strain. So upon an external field as high as 50 kOe, this kind of balance will be broken in favor of enhancing FM fraction.

As a result, $M_{FC}-M_{ZFC}$ is relatively larger in the middle composition range, as shown in Fig. 3(a). As to the case of the low magnetic field as 10 Oe, because the transition from monoclinic phase to orthorhombic phase after FC process should be negligible,[18,19] small values of $M_{FC}-M_{ZFC}$ could be expected. However, for $x \geq 0.90$, the $M_{FC}-M_{ZFC}$ value of 10 Oe is a little higher than that of 50 kOe. It is not surprising for a material with a long-range FM ordering because both FC and ZFC magnetizations are saturated under 50 kOe, giving rise to a small difference between them, and accordingly, to a suppressed T_{irr}. Also, due to the trend of magnetization toward saturation at 50 kOe, the corresponding value of $(M_{FC}-M_{ZFC})/M_{ZFC}$ is much less than at 10 Oe, as shown in Fig. 3(b).

C. Phase diagram

Figure 5 shows a modified phase diagram for $Sm_{1-x}Ca_xMnO_3$ ($0.80 \leq x \leq 0.92$) according to the character-
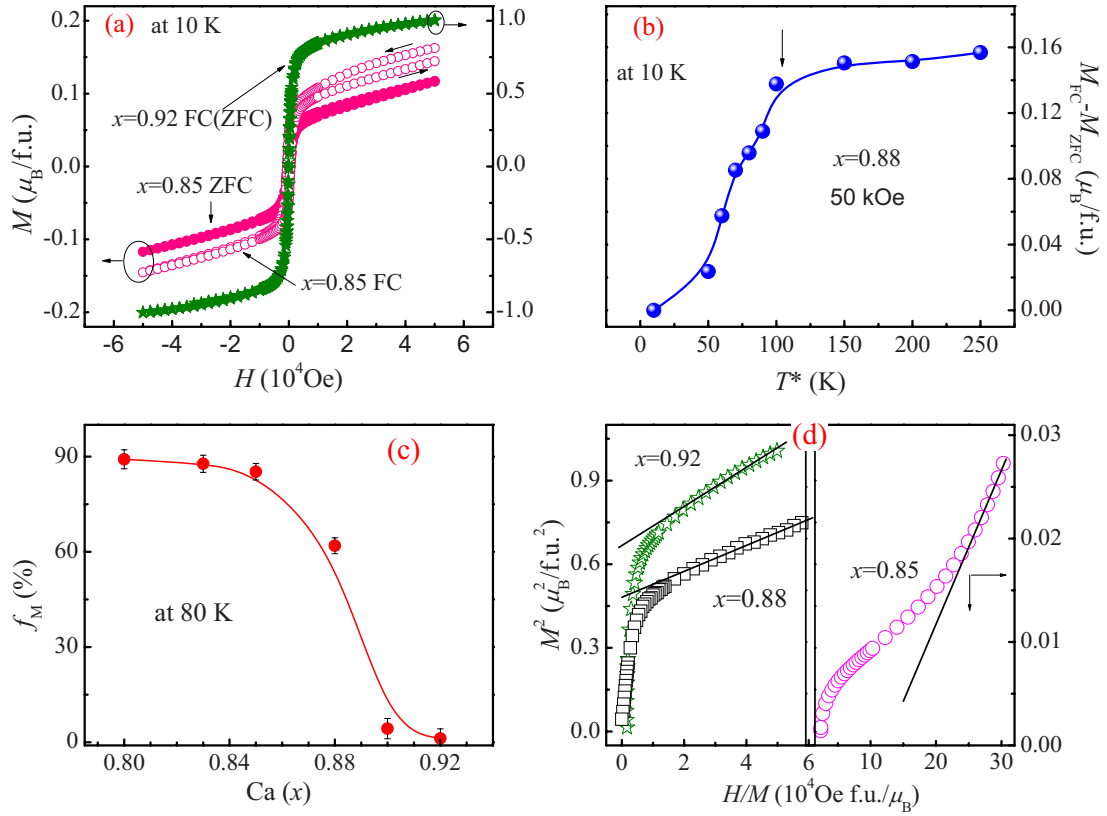
FIG. 4. (Color online) (a) Magnetic field cycling of magnetization under both FC (50 kOe→−50 kOe→+50 kOe) and ZFC (0→ +50 kOe→−50 kOe→+50 kOe.) modes for $x=0.88$ and 0.92. (b) Difference in M between FC and ZFC modes as a function of temperature T^* for $x=0.88$ (see text for the definition of T^*). The data in both modes used correspond to the end point of a complete magnetic field cycling in $M(H)$ curve at 10 K. (c) x dependent monoclinic phase fraction (f_M) with error bars obtained from the refinement of x-ray data at 80 K. (d) Arrott plots at 10 K for $x=0.85$, 0.88, and 0.92. The solid lines in (b) and (c) are guides for the eyes, but in (d), the solid line is a linear extrapolation.

istic temperatures mentioned above. As to T_{irr}, only those at 10 Oe are plotted because the intrinsic properties such as the accommodation strain will be obscured under a high magnetic field such as 50 kOe. Two distinct features can be found in Fig. 5. One is a rectanglelike region of the Griffiths phase for $x \geq 0.85$ as emphasized by the red hatched zone, which is quite different from the triangle-shape region of Griffiths phase in hole-doped manganite $La_{1-x}Sr_xMnO_3$ and $La_{1-x}Ba_xMnO_3$.[12,14] Another is an irreversibility line (formed by T_{irr}) in the whole composition range, which drills through the region of Griffiths phase.

On $x \geq 0.85$ side of the phase diagram, the TMI line may be a hint of certain correlations between low-temperature glassy state and high-temperature "cluster" state, namely, Griffiths phase. As we discussed above, the TMI behavior suggests the existence of the strain accommodation at low temperatures in the present system. So the irreversibility line across over the region of Griffiths phase in Fig. 5 reflects that the effect of strain extends to the temperatures above T_C. This behavior is reminiscent of the precursor embryonic fluctuations above the martensitic transition temperature observed in other martensites.[30]

It suggests that the Griffiths phase in present system is correlated with the strain field, possibly in its initial state. On the other side of the phase diagram with $x \leq 0.83$, the TMI

line is below the $T_N(C)$ line. So the existence of possible Griffiths phase will be overcasted by the overwhelming C-AFM correlations, as shown in Fig. 2(a), though the TMI line may imply the onset of nucleation of FM clusters. It is
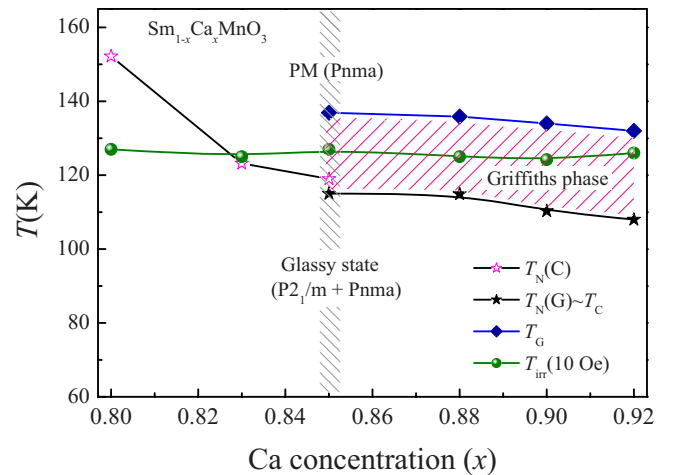

FIG. 5. (Color online) A modified phase diagram of $Sm_{1-x}Ca_xMnO_3$ ($0.80 \leq x \leq 0.92$). The hatched zones around 0.85 and above 0.85 represent the region of CMR (black) and Griffiths phase (red), respectively. The solid lines are guides for the eyes.

similar to what we observed in $La_{0.15-x}Y-xCa_{0.85}MnO_3$, i.e., the Griffiths phase occurs only in samples with a well reduced $T_N(C)$.[16] This kind of correlation between the Griffiths and C-AFM phases can be readily understood in that the latter corresponds to the monoclinic crystal structure, which is more distorted than orthorhombic one, consequently harmful to the nucleation of FM clusters, thus, to the emergence of Griffiths phase.

Generally, in hole-doped (bilayered) manganites, the Griffiths phase can be understood in terms of the intrinsic inhomogeneity induced by the quenched disorders.[12,15] Because of the similar ionic size of Ca^{2+} and Sm^{3+}, and the feature of slightly doping, the present system should belong to the type of weakly disordered manganites.[31] In the weakly disordered system, the accommodation strain rather than the quenched disorder is considered to be responsible for the intrinsic inhomogeneity or phase separation.[4] Moreover, the glassy state in weakly distorted manganites has been argued not to be a canonical "spin glass" in which the quenched disorder is necessary, but to be a structure glass in which the accommodation strain is a key element.[21] Therefore, it implies that in the present system, the strain field might account for the electronic phase separation in a well-extended temperature range, namely, the Griffiths phase above T_C, as well as the glassy behavior at the low temperatures. Even so, it is too arbitrary to ascribe the Griffiths phase to the accommodation strain since the contribution from quenched disorders cannot be thoroughly excluded at present. Consequently, more efforts from both experimental and theoretical sides are desired in order to clarify the nature and the origin of Griffiths phase in the electron-doped manganites.

As displayed in Fig. 5, the CMR effect happens in a quite localized region near $x=0.85$ (black hatched zone), while the Griffiths phase behavior exists in a well extended composition range, namely, $0.85 \leq x \leq 0.92$. Despite the fact that CMR occurs on the boundary of the region of the Griffiths phase, it is clear that Griffiths phase only is insufficient to expect the emergence of CMR.

IV. CONCLUSION

The magnetic properties of slightly electron-doped $Sm_{1-x}Ca_xMnO_3$ $(0.80 \leq x \leq 0.92)$ have been investigated. A distinct character of the Griffiths phase was found in inverse magnetic susceptibility for $x \geq 0.85$ above Curie temperature. TMI observed in all samples is suggested to correspond to the accommodated strain arising from martensitelike phase transition. The low-field TMI line passes through the region of the Griffiths phase in the modified phase diagram. This result links the Griffiths phase with the strain field, probably indicating an alternative approach of understanding the Griffiths phase in the electron-doped manganites. In addition, as indicated by the phase diagram, the Griffiths phase is not necessary to be tied with the CMR in the electron-doped manganites.

[1] *Colossal Magnetoresistance, Charge Ordering, and Related Properties of Manganese Oxides*, edited by C. N. R. Rao and B. Raveau (World Scientific, Singapore, 1998).

[2] E. Dagotto, New J. Phys. **7**, 67 (2005).

[3] E. Dagotto, T. Hotta, and A. Moreo, Phys. Rep. **344**, 1 (2001).

[4] K. H. Ahn, T. Lookman, and A. R. Bishop, Nature (London) **428**, 401 (2004).

[5] P. R. Sagdeo, Shahid Anwar, and N. P. Lalla, Phys. Rev. B **74**, 214118 (2006).

[6] S. Hebert, A. Maignan, V. Hardy, C. Martin, M. Hervieu, B. Raveau, R. Mahendiran, and P. Schiffer, Eur. Phys. J. B **29**, 419 (2002).

[7] R. B. Griffiths, Phys. Rev. Lett. **23**, 17 (1969).

[8] J. Burgy, M. Mayr, V. Martin-Mayor, A. Moreo, and E. Dagotto, Phys. Rev. Lett. **87**, 277202 (2001).

[9] A. H. Castro Neto, G. Castilla, and B. A. Jones, Phys. Rev. Lett. **81**, 3531 (1998).

[10] M. Randeria, J. P. Sethna, and R. G. Palmer, Phys. Rev. Lett. **54**, 1321 (1985).

[11] W. Jiang, X. Zhou, G. Williams, Y. Mukovskii, and K. Glazyrin, Phys. Rev. Lett. **99**, 177203 (2007).

[12] J. Deisenhofer, D. Braak, H. A. Krug von Nidda, J. Hemberger, R. M. Eremina, V. A. Ivanshin, A. M. Balbashov, G. Jug, A. Loidl, T. Kimura, and Y. Tokura, Phys. Rev. Lett. **95**, 257202

(2005).

[13] M. B. Salamon, P. Lin, and S. H. Chun, Phys. Rev. Lett. **88**, 197203 (2002).

[14] Wanjun Jiang, X. Z. Zhou, G. Williams, Y. Mukovskii, and K. Glazyrin, Phys. Rev. B **77**, 064424 (2008).

[15] R. F. Yang, Y. Sun, W. He, Q. A. Li, and Z. H. Cheng, Appl. Phys. Lett. **90**, 032502 (2007).

[16] T. Qian, P. Tong, B. Kim, S. I. Lee, N. Shin, S. Park, and B. G. Kim, Phys. Rev. B **77**, 094423 (2008).

[17] C. L. Lu, K. F. Wang, S. Dong, J. G. Wan, J.-M. Liu, and Z. F. Ren, J. Appl. Phys. **103**, 07F714 (2008).

[18] M. Respaud, J. M. Broto, H. Rakoto, J. Vanacken, P. Wagner, C. Martin, A. Maignan, and B. Raveau, Phys. Rev. B **63**, 144426 (2001).

[19] R. Mahendiran, A. Maignan, C. Martin, M. Hervieu, and B. Raveau, Phys. Rev. B **62**, 11644 (2000).

[20] C. Magen, P. A. Algarabel, L. Morellon, J. P. Araujo, C. Ritter, M. R. Ibarra, A. M. Pereira, and J. B. Sousa, Phys. Rev. Lett. **96**, 167201 (2006).

[21] W. D. Wu, C. Israel, N. Hur, S. Park, S.-W. Cheong, and A. D. Lozanne, Nat. Mater. **5**, 881 (2006).

[22] K. Binder and A. P. Young, Rev. Mod. Phys. **58**, 801 (1986).

[23] V. Moshnyaga, B. Damaschke, O. Shapoval, A. Belenchuk, J. Faupel, O. I. Lebedev, J. Verbeeck, G. Van Tendeloo, M. Mück-

sch, V. Tsurkan, R. Tidecks, and K. Samwer, Nat. Mater. **2**, 247 (2003).

[24] T. Qian, G. Li, T. Zhang, T. F. Zhou, X. W. Kang, and X. G. Li, Phys. Rev. B **76**, 014433 (2007).

[25] C. Martin, A. Maignan, F. Damay, M. Hervieu, B. Raveau, Z. Jirak, G. Andre, and F. Bouree, J. Magn. Magn. Mater. **202**, 11 (1999).

[26] V. Podzorov, B. G. Kim, V. Kiryukhin, M. E. Gershenson, and S-W. Cheong, Phys. Rev. B **64**, 140406(R) (2001).

[27] Zenji Nishiyama, in *Martensitic Transformation*, edited by M. Fine, M. Meshii, and C. Wayman (Academic, New York, 1978).

[28] G. R. Barsch, B. Horovitz, and J. A. Krumhansl, Phys. Rev. Lett. **59**, 1251 (1987).

[29] M. Hervieu, A. Barnabe, C. Martin, A. Maignan, F. Damay, and B. Raveau, Eur. Phys. J. B **8**, 31 (1999).

[30] H. Seto, Y. Noda, and Y. Yamada, J. Phys. Soc. Jpn. **59**, 978 (1990).

[31] Y. Tomioka and Y. Tokura, Phys. Rev. B **70**, 014432 (2004).